ORGANIC CHEMISTRY FRONTIERS

RESEARCH ARTICLE

View Article Online
View Journal | View Issue

Cite this: *Org. Chem. Front.*, 2025, **12**, 6450

Manipulating stereo-communication in binaphthol-bridged α- and β-cyclodextrins to develop β-selective chiroptical pH switching and anion sensing in water

Giovanni Preda,[a,b] Sonia La Cognata,[a] Laura Pedraza-González,[c] Laurine Carlier,[b] Maxime Kolb,[b] Gennaro Pescitelli,[c] Valeria Amendola,[a] Dominique Armspach *[b] and Dario Pasini *[a]

Received 19th June 2025,
Accepted 15th August 2025

DOI: 10.1039/d5qo00910c

rsc.li/frontiers-organic

Molecular structures comprising naturally-occurring, stereodefined cyclodextrins and binaphthyls as bridging units have been realized, designed in such a way that the stereocommunication mode between the two chiral entities is unfavourable ('chiral mismatch'). The induced strain translates into highly responsive chiroptical behavior. On one side, the binaphthol-containing structure functions as a pH-controlled, single-molecule chiroptical switch, with reversal of the optical activity from acidic to basic conditions in a fully reversible manner. Additionally, the same host molecule demonstrates a pronounced chiroptical response to perrhenate in aqueous solution at pH 2.5, showing excellent selectivity for this specific anion. Computational analysis confirmed that the major effect of ReO_4^- complexation is making new conformations accessible to the binaphthol moiety with a large variation of the associated dihedral angles.

Introduction

Supramolecular engineering of confined, chiral nano-spaces in the fields of sensing, optoelectronics and catalysis is a subject of growing interest.[1] In this regard, the naturally occurring and optically active cyclodextrins (CDs) are of great significance, as they can form inclusion complexes with a large variety of molecules in water by virtue of their hydrophobic cavity. This unique property has been increasingly exploited over the last century for a variety of purposes, ranging from food and pharmaceutical applications to detergents, pollutant removal and catalysis among others.[2]

Parallel to these developments is the growing interest in chiroptical materials, in view of their possible applications in fields such as smart optoelectronics, data encryption, and biochemical assays.[3–5] Sustainability concerns have driven the search for new strategies aiming at transferring the non-chromophoric chirality found in affordable, naturally occurring molecules of the "chiral pool", to organic chromophores with strong chiroptical properties. In this regard, CDs have the potential to serve as excellent starting materials for developing chiral functional organic materials. However, their effectiveness in inducing chirality transfer has rarely been reported.[6–10]

Recently, we demonstrated that stereo-communication between *point-chiral* permethylated α- and β-CDs and *axially-chiral* atropoisomeric biphenol bridging units (Fig. 1, top) can be highly effective.[11] In such two-level molecular systems, the stereochemical information of the non-chromophoric CD (point chirality) is transferred to the chromophoric biphenyl capping unit (axial chirality), imposing a single axial configuration on an otherwise *stereodynamic* cap.† The CDs impose either (a*R*) or (a*S*) configurations on the biaryl axis depending on the presence or absence of intramolecular hydrogen bonding. In the case of a 2,2′-dimethoxy-1,1′-biphenyl unit, where such hydrogen bonds are absent, the atropoisomeric unit adopts an (a*R*) configuration. On the other hand, when OH groups are present, intramolecular hydrogen bonds rigidify the 2,2′-dihydroxy-1,1′-biphenyl bridging unit, selecting the (a*S*) configuration on the biaryl axis.

Stereostable, axially chiral chromophoric units can also possess valuable properties in the field of chiroptical sensing. In substituted 1,1′-binaphthyl derivatives, the expression of chirality – the asymmetry induced by the stereogenic axis – is

[a]*Department of Chemistry and INSTM Research Unit, University of Pavia, 27100 Pavia, Italy. E-mail: dario.pasini@unipv.it*
[b]*Équipe Confinement Moléculaire et Catalyse, Université de Strasbourg, Institut de Chimie de Strasbourg, UMR 7177 CNRS, 4 rue Blaise Pascal, CS90032, 67081 Strasbourg Cedex, France. E-mail: d.armspach@unistra.fr*
[c]*Department of Chemistry and Industrial Chemistry, University of Pisa, via Moruzzi 13, 56124 Pisa, Italy*

†The aryl–aryl bond in the biphenol unit is typically freely rotating at room temperature when not part of a capping unit.

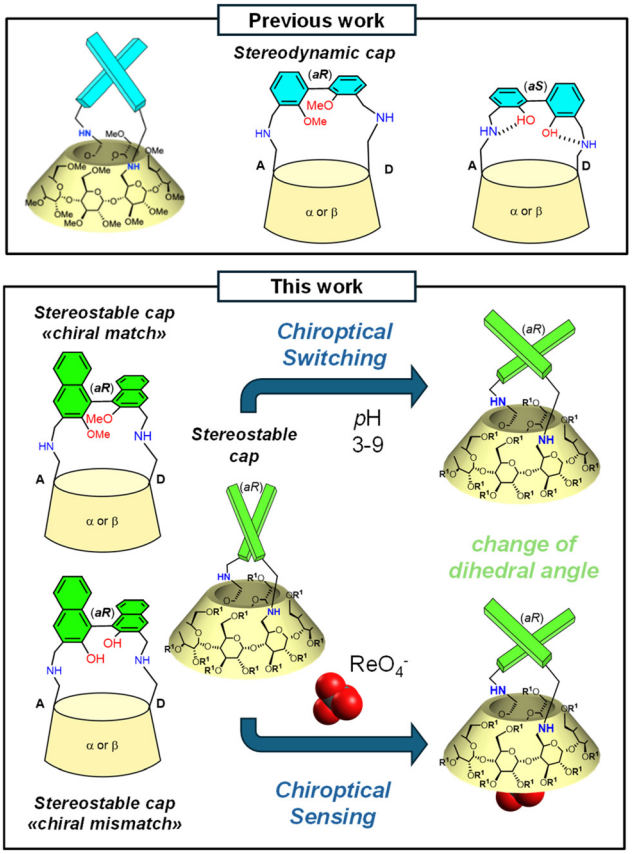

Fig. 1 Previously reported biphenyl-capped CDs *vs.* binaphthyl-capped CDs reported in this work, and their sensing and switching behaviour.

directly embedded into the two π-extended chromophoric regions. Their use in chiroptical sensing has recently been successfully exploited by our groups and others, given that only slight changes in the dihedral angle between the two naphthyl rings lead to a significant modulation of the ECD signal.[12]

We hypothesized that bridging CDs with *stereostable* atropoisomeric units (Fig. 1, bottom) instead of *stereolabile* biphenolic ones, might induce substantial chiroptical modulation in response to guest complexation and/or an external stimulus, particularly when creating a "chiral mismatch" in the two stack molecular systems. In essence, we envisioned that bridging the CDs with a stereostable (a*R*) 2,2′-dihydroxy-1,1′-binaphthyl would create strain in the bridged CD as it deviates from the preferred (a*S*) configuration.

Any release of this strain caused by a change in the binaphthyl dihedral angle would lead to a significant modulation of the ECD signal. In this article, we present the synthesis and chiroptical characterization of axially chiral, enantiostable binaphthyl-bridged α- and β-CDs and demonstrate their application as chiroptical pH switches and chiroptical sensors, selective for the ReO_4^- anion, in aqueous solution.

Results and discussion

Synthesis

Binaphthol-bridged CDs **1a,b** and **2a,b** were synthesized from permethylated A,D-diamino α- and β-CDs,[13a,b] and respectively enantiopure (a*R*)-3,3′-diformyl-2,2′-dimethoxy-1,1′-binaphthyl and (a*R*)-3,3′-diformyl-2,2′-dihydroxy-1,1′-binaphthyl (Scheme 1),

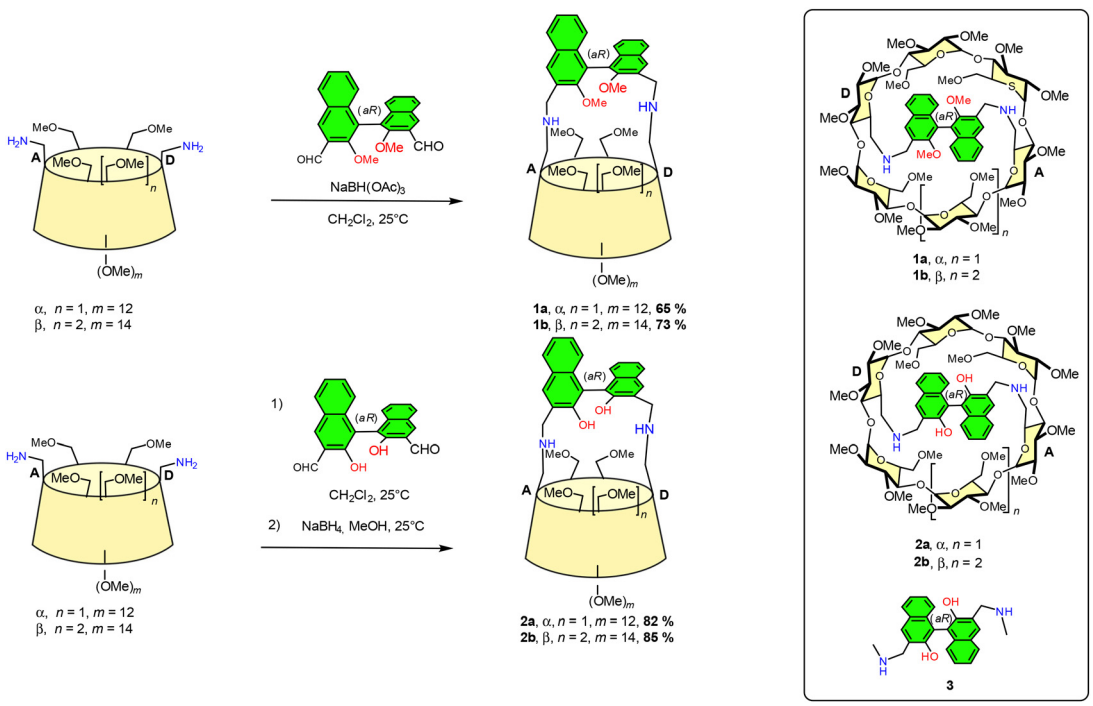

Scheme 1 Synthesis of binaphthol-capped α- and β-CDs.

following the procedures optimized for their biphenol analogues. While one-pot reductive amination was used for accessing 2,2′-dimethoxy-1,1′-binaphthyl-bridged CDs **1a,b**, a two-step procedure involving a condensation step followed by reduction of the diimine intermediate with $NaBH_4$ was necessary for synthesizing **2a,b**. This difference of reactivity can be attributed to the key role played by the intramolecular hydrogen bonding of the phenolic groups in stabilizing the neighbouring imine nitrogen atoms, which makes the reduction of the diimine more challenging in the case of **2a,b**.

Remarkably, the CD truncated cone is sufficiently flexible to ensure efficient bridging, even in the case of the hydroxy derivatives, where the (a*R*) axial configuration of the binaphthyl cap is not the most suited for the CD unit.

The cavity-free analogue **3** was synthesized from 3,3′-diformyl-2,2′-dihydroxy-1,1′-binaphthyl and methylamine by adapting a reported procedure.[14] All new compounds were extensively characterized by high-resolution mass spectrometry as well as mono- and bidimensional NMR spectroscopy, confirming the expected C_2-symmetry of the α-CD derivatives (see SI). Unlike **1a** and **1b**, the exchangeable protons (NH and OH) could not be revealed in neither **2a** nor **2b** when their ^{1}H NMR spectra were recorded in $CDCl_3$. To detect these protons and gain more information on possible intramolecular OH···NH or/and OH···O hydrogen bonds, variable temperature (VT) NMR studies on both compounds were performed in CD_2Cl_2. At 298K, the spectrum of **2a** displays a broad singlet at δ = 4.58 ppm integrating for four protons, consistent with both OH and NH protons (Fig. S1). Upon cooling to 283K, this signal broadens and is significantly downfield shifted ($\Delta\delta$ = 0.25 ppm) (Fig. S2). Instead, a CD_2Cl_2 solution of **2b** does not reveal any exchangeable protons (Fig. S3) at 298 K; upon cooling, a broad singlet at δ = 10.60 ppm, integrating for about two protons and most likely corresponding to the two OH protons, emerges at 243K and is the sharpest at 223K (Fig. S4 and S5). The signal is downfield shifted from 233K to 193K ($\Delta\delta$ = 0.68 ppm). Furthermore, unlike all other aromatic protons, the H-8,8′ binaphthyl protons of both **2a** (Fig. S6) and **2b** (Fig. S7) are remarkably upfield shifted ($\Delta\delta$ = 0.09 ppm for **2a** and 0.12 and 0.08 ppm for **2b**) upon cooling. Clearly, in both compounds, intramolecular hydrogen bonds involving the NH and OH functionalities, the strength of which is temperature dependant,[11] have a strong impact on the binaphthyl dihedral angle (see below).

Attempts to obtain single crystals suitable for X-ray crystallography were unsuccessful, but in-depth insights into the molecular structure of the bridged CDs were gained through molecular modelling (see Computational studies below).

Optical and chiroptical characterization and pH switching behaviour

UV-vis and ECD spectra of all molecules were initially recorded in both protic (water and methanol) and aprotic (acetonitrile) solvents to assess the impact of potential intramolecular hydrogen bonds (HN···HO– and OH···O) between the two components of the bridged CDs (CD and binaphthyl units). All spectra are dominated by the binaphthyl chromophoric moiety, exhibiting maximum absorbance in the UV region at 230 nm for all compounds (Fig. S8 and S9). Regarding the methoxy derivatives **1a** and **1b**, where the chiral units (CD and binaphthyl) match, no significant differences in the ECD spectra were observed regardless of the solvent used (Fig. S8, S9 and Fig. 2). These compounds display the characteristic bisignate excitonic couplet centered at 230 nm, typical of the binaphthyl system. In contrast, for the hydroxyl derivatives **2a** and **2b**, which exhibit a "chiral mismatch", significant differences were observed, particularly for **2b**. The negative portion of the bisignate excitonic couplet in the ECD spectra of **2b**, centered at 234 and 237 nm in MeOH and ACN respectively, is almost completely suppressed in H_2O (Fig. 2), while a new bisignate excitonic couplet of opposite sign emerges at 224 nm. For **2a** (Fig. S2), a partial decrease in optical activity is observed, although the exciton couplet retains the same sign when switching from organic solvents to water.

We first investigated whether the protonation state of the amino groups near the binaphthyl chromophore could influence the chiroptical properties of **2b**. Because of the low solubility of **2b** in water near neutral pH at concentrations suitable for potentiometric studies, these titrations were conducted in an EtOH/H_2O (3 : 2, v/v) mixture. The distribution diagram (Fig. S10), calculated from the protonation constant values, indicates that compound **2b** is predominantly (>90%) in its bis-protonated form $[H_2(\mathbf{2b})]^{2+}$ between pH 2 and 4 (pK_{a1} = 5.66 ± 0.08), with both amine groups near the binaphthyl moiety in the protonated form. For pH values above 5, the con-

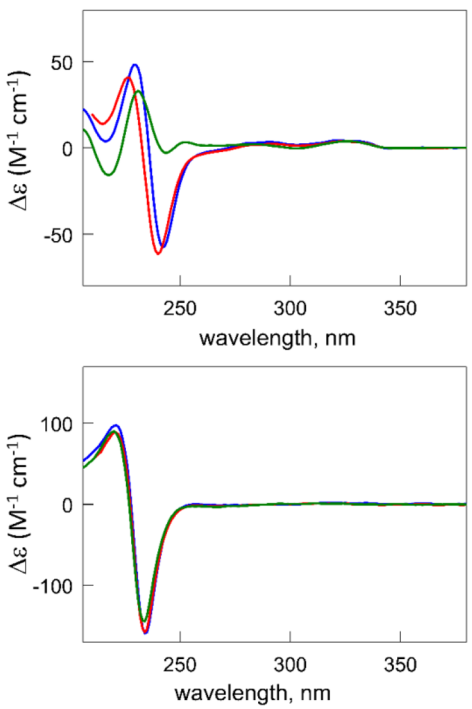

Fig. 2 ECD spectra of **2b** (top) **1b** (bottom) and recorded in different solvents: acetonitrile (blue), MeOH (red) and water (green).

centration of the mono-protonated species $[H(\mathbf{2b})]^+$ increases, reaching its maximum abundance around pH 6.2 (pK_{a2} = 7.00 ± 0.02). At approximately neutral pH, the solution contains an almost equimolar mixture of the mono-protonated and neutral forms, $[H(\mathbf{2b})]^+$ and **2b**, while the free amine species **2b** predominates in solution above pH 7.5.

The effect of the protonation was further investigated by recording the ECD spectra of **2b** in H_2O at varying pH values. Remarkably, as the pH increased from 3 to 9 (Fig. 3, top), the ECD spectrum underwent a nearly complete inversion. Specifically, the exciton couplet centered at 230 nm, observed at pH 3 and attributed to the bis-protonated species $[H_2(\mathbf{2b})]^{2+}$, gradually diminished with increasing pH and was ultimately replaced by a new couplet of opposite sign at pH 9, where the gradual deprotonation of $[H_2(\mathbf{2b})]^{2+}$ and the formation of the free base **2b** occurs. The profiles of the pH-dependent UV/vis spectra (Fig. S11) revealed only a small reduction of the intensity of the main absorption band at 230 nm, confirming the absence of deprotonation of the OH groups in the pH range 3–9. It is known that the ECD spectra of binaphthyl systems are highly sensitive to the dihedral angle between the two planes defined by the naphthyl fragments. Even minor angle changes can significantly alter the ECD spectrum and may even lead to a complete sign inversion, despite the chromophore retaining its original axial configuration.[15]

Whereas other examples of molecular systems with pH-dependent ECD reversible modulation have been reported,[16,17] the present case represents, to our knowledge, the only example of a quasi-complete optical inversion triggered by pH changes. This behaviour is completely reversible and reproducible. Upon successive additions of concentrated acid and base solutions to the same aqueous solution of **2b**, ten complete cycles of ECD inversion between pH 3 and 9 (Fig. 3, bottom) were carried out without any detectable loss of optical activity. This makes **2b** one of the few known single-molecule chiroptical switch that operates in water and is capable of reversibly switching the optical activity of the binaphthyl exciton couplet in response to acid–base stimuli, in a fully reversible, hysteresis-free and non-destructive manner. The protonation state of the amine groups neighbouring the binaphthyl systems exerts a change in the dihedral angle through a buttressing effect,[18] amplified by the intramolecular strain introduced by the atropoisomeric binaphthyl cap in a 'chiral mismatch' with the cyclodextrin cavity and by the influence of intramolecular hydrogen bonds. Indeed, as a control, the pH-dependent ECD spectra of model compound **3** (Fig. S12) showed only a modest reduction in the intensity of the excitonic couplet, with no spectral inversion.

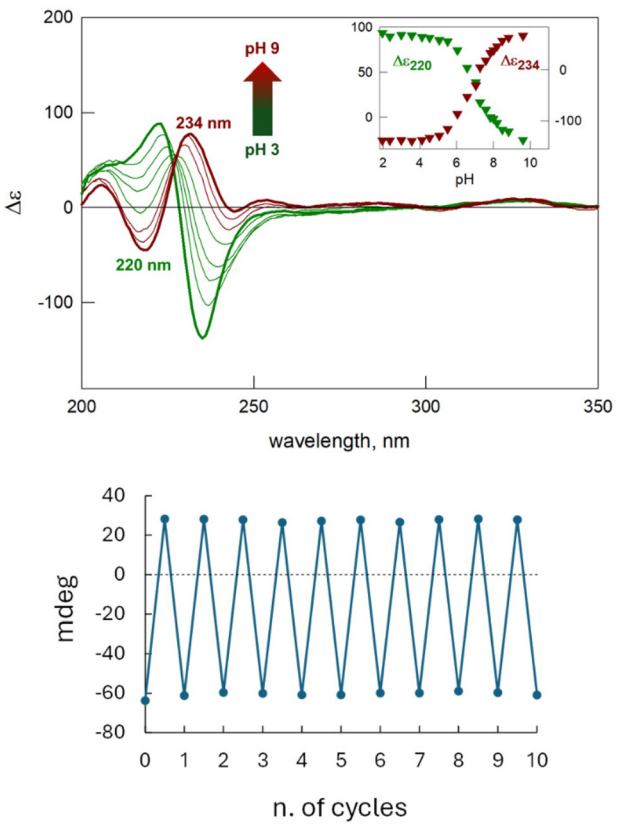

Fig. 3 Top: potentiometric titration of **2b** (1 × 10^{-5} M) in H_2O monitored by ECD (0.025 M $NaNO_3$, path length 0.1 cm). Inset: the ECD titration profiles ($\Delta\varepsilon$ *vs.* pH) at 220 nm and 234 nm, represented by green and dark red symbols. Bottom: ECD values recorded at 234 nm over *n* complete cycles of successive additions of concentrated acid and base solutions to the same H_2O solution of **2b** (see SI for details).

Chiroptical sensing

The ability of CDs – whether in their native state or permethylated as in the present case – to encapsulate a wide range of organic species in aqueous solution arises from their unique structure, which features a hydrophobic inner cavity as well as a hydrophilic outer surface. The hydrophobic cavity facilitates the encapsulation of poorly water-soluble organic guests, while the hydrophilic exterior ensures the solubility of the resulting inclusion complexes in water.

We sought to explore the potential of **2b** as a chiroptical sensor for anions with a known degree of hydrophobicity. Studies by Beer *et al.*[19] on CDs equipped with halogen or hydrogen bond donors at the primary face have shown that such hosts can selectively bind the hydrophobic ReO_4^- anion in water. This anion is of particular interest as a non-radioactive surrogate for the radioactive pollutant TcO_4^-.

We have recently demonstrated[20] that incorporating a binaphthyl moiety into a hexa-protonated azacryptand enables the resulting cage-like host to act as a selective chiroptical chemosensor for ReO_4^- in acidic aqueous solution.[21,22] A similar approach was employed for **2b**. Anion-binding titration experiments were carried out in aqueous solution acidified to pH 2.5 to ensure full protonation of the amine groups. Under these conditions, the addition of $NaReO_4$ to a 0.1 mM solution of the bis-protonated host, $[H_2(\mathbf{2b})]^{2+}$, led to a significant modulation of the binaphthyl exciton couplet centered around 230 nm, particularly in the regions near 234 nm and 223 nm (Fig. 4, top). Specifically, the intensities of the couplet bands decreased progressively until reaching a plateau upon addition

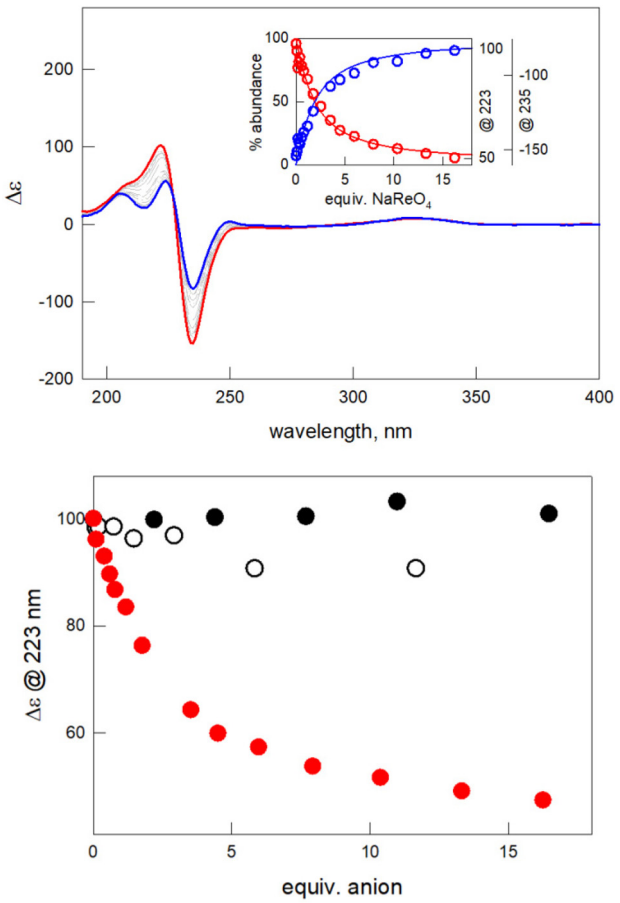

Fig. 4 Top: titration of $[H_2(\mathbf{2b})]^{2+}$ with $NaReO_4$ monitored by ECD in aqueous solution (the red and blue lines correspond to initial and final ECD spectra, respectively). The inset shows the experimental titration profiles ($\Delta\varepsilon$ *vs.* equivalents of the added $NaReO_4$) at 234 nm and 223 nm (blue and red circles, respectively). The titrations profiles are overlaid with the distribution curves (% abundance *vs.* equivalents of titrant) for the 1 : 1 complex formed between $[H_2(\mathbf{2b})]^{2+}$ and perrhenate (log K = 3.80; red line, free host; blue line 1 : 1 complex). Bottom: ECD titration profiles of $[H_2(\mathbf{2b})]^{2+}$ (1.03×10^{-4} M) with three different anions, perrhenate, iodide and sulfate (red, white and black symbols, respectively) as sodium salts, in acidic water (TFA) at pH 2.5 (path length = 0.1 cm, $\Delta\varepsilon$ measured at 223 nm).

of excess $NaReO_4$, and the high-energy branch split in two distinct bands. These changes support the hypothesis that perrhenate is encapsulated within the β-CD cavity, where it changes its conformation and that of the binaphthyl moiety. Analysis of the titration data, assuming a 1 : 1 $[H_2(\mathbf{2b})]^{2+}/ReO_4^-$ binding stoichiometry, yielded an association constant of 3.80 (3) log units (inset, Fig. 4, top). Remarkably, this value is one order of magnitude higher than that observed by Beer for his best performing system.[19] From the analysis of the linear portion of the titration curve, the limits of detection (LOD) and quantification (LOQ) were determined, and were found to be 18 μM and 60 μM, respectively (see the SI for details).

The chiroptical response of $[H_2(\mathbf{2b})]^{2+}$ to various anions was further tested against a series of other species (ClO_4^-, OTf^-, NO_3^-, Cl^-, Br^-, I^- and SO_4^{2-}; see Fig. S13 and S22). Among these, only ClO_4^- (Fig. S13 and S14) and OTf^- (Fig. S15 and S16) induced notable modulation of the ECD spectrum of $[H_2(\mathbf{2b})]^{2+}$ (Fig. S21). The corresponding 1 : 1 binding constants were found to be 2.44(5) and 2.48(1) log units for ClO_4^- and OTf^-, respectively—at least one order of magnitude lower than that observed for perrhenate (Table S1). To demonstrate that the strong chiroptical response of **2b** to ReO_4^- is directly linked to its unique structural features, we conducted control ECD studies with perrhenate on three related compounds: **1b**, **2a**, and **3** (Fig. S22). No chiroptical changes were observed in the ECD spectra upon the incremental addition of $NaReO_4$ to an aqueous solution of the cavity-free compound **3**.

Furthermore, only small changes were recorded for systems featuring either a smaller cyclodextrin cavity with hydroxyl groups (**2a**) or a comparable β-CD cavity bearing protected hydroxyl groups (**1b**). These results clearly indicate that both the size of the cyclodextrin cavity and the presence of intramolecular hydrogen bonding between the CD unit and the binaphthyl bridge – which is absent in the dimethoxy host **1b** – are essential for an effective chiroptical response to perrhenate in aqueous solution.

The formation of a 1 : 1 complex with ReO_4^- was also confirmed by ^{1}H NMR titration (Fig. 5 and Fig. S23). The association constant (3.93(7) log units) is consistent with the value obtained from ECD titration. Upon addition of $NaReO_4$ to an acidic solution of the host in D_2O (pD adjusted to 2.5 with TFA), the 6-OMe singlets were significantly affected: two shifted downfield, while the remaining three shifted upfield (see white and black symbols in Fig. 5, and titration profiles in Fig. S24). In addition to the 6-OMe signals, only a few other resonances were influenced by complexation—specifically, the Hε proton of the binaphthyl moiety and two of the seven anomeric (H-1) protons (Fig. S23). Given that the chemical shifts of H-1 protons are highly sensitive to conformational changes in cyclodextrins, these results suggest that ReO_4^- binding induces a conformational rearrangement in the two glucose units associated

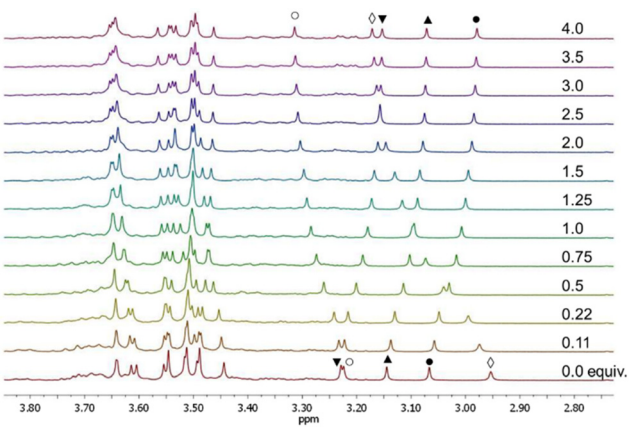

Fig. 5 Zoom of the aliphatic region of ^{1}H-NMR spectra (400 MHz) taken over the course of the titration of **2b** (0.5 mM in D_2O pD = 2.5 with CF_3COOH) with a solution of $NaReO_4$.

with the shifted H-1 protons – possibly those directly linked to the binaphthyl bridge. By using triflic acid instead of trifluoroacetic acid as the acidic medium, the binding affinity of $[H_2(\mathbf{2b})]^{2+}$ with ReO_4^- could be confirmed through a ^{1}H-NMR titration experiment (Fig. S25 and S26).

The competition of OTf^- and Cl^- with ReO_4^- for binding to the host was also investigated through ECD titrations in aqueous solution. These experiments were carried out using either triflic acid or HCl, instead of TFA, for the preparation of both the $[H_2(\mathbf{2b})]^{2+}$ (0.1 mM) and ReO_4^- solutions at pH 2.5. Under these conditions, the concentration of either competitor of OTf^- and Cl^- was in significant excess (~30 : 1 molar ratio) relative to the $[H_2(\mathbf{2b})]^{2+}$ host. However, these studies indicated that, even in presence of competing species, perrhenate binding induces significant changes in ECD spectra of the host. From the fitting of the titration profiles, we could also determine the binding constant for ReO_4^- under these conditions (see Table S2 and Fig. S27, S28). As expected, in OTf^- containing medium, the binding constant for ReO_4^- was about 3.5 times lower than that calculated in TFA at the same pH.

Computational studies

To interpret the ECD properties of binaphthol-bridged CDs and substantiate their anion sensing ability, a computational study was run on compound **2b** and its complex with ReO_4^-, following the same approach employed in our previous work on CD's capped with 2,2′-dihydroxy-1,1′-biphenyl units.[11]

Classical explicit-solvent molecular dynamics (MD) simulations were carried out for $[H_2(\mathbf{2b})]^{2+}$ (**2b** in acidic conditions) in the presence of two equivalents of either Cl^- (**MD1**) or ReO_4^- (**MD2**), enabling a comparative assessment of how these anions influence the conformational dynamics of the host. We focused on two structural parameters: (i) the dihedral angle (θ) between the naphthyl planes of the binaphthol unit, serving as a local flexibility indicator, and (ii) the root-mean-square deviation (RMSD) of the CD scaffold, as a global stability indicator.

In the presence of Cl^- (**MD1**), θ remained confined to a relatively narrow window (−75° to −95°) throughout the 1.2 μs trajectory (Fig. S29), with the system ultimately settling at −75° after ~900 ns and remaining stable thereafter. This behavior suggests restricted torsional freedom of the binaphthol unit, consistent with a lack of directional non-covalent interactions. However, the CD scaffold itself exhibited significant conformational fluctuations, with RMSD values frequently exceeding 2.5 Å (Fig. S30), indicating limited global stabilization by Cl^-, acting only as a charge-balancing ion.

In contrast, the behavior of $[H_2(\mathbf{2b})]^{2+}$ in the presence of ReO_4^- (**MD2**) was markedly different. The inter-naphthyl angle explored a broader range (−80° to −110°) across a longer 2.0 μs simulation (Fig. 6b), revealing that ReO_4^- ion promotes access to binaphthyl conformers not sampled in the Cl^- simulation.

This enhanced local flexibility suggests a dynamic interplay between the binaphthol moiety and the ReO_4^- anion. Distinct structural states associated with θ values of −81°, −90°, and −110° were captured for further analysis (see colored stars in Fig. 6b).

These findings underscore the dynamic nature of the $[H_2(\mathbf{2b})]^{2+}\cdot ReO_4^-$ complex and highlight the role of ReO_4^- in expanding the accessible conformational space. A key mechanistic feature appears to be water-mediated hydrogen bonding between ReO_4^- and the binaphthol hydroxyl groups (Fig. 6c–e). These solvent bridges form a dynamic coordination network that alleviates torsional constraints on the binaphthol moiety while maintaining overall host integrity. Despite the enhanced local motion, the $[H_2(\mathbf{2b})]^{2+}\cdot ReO_4^-$ system exhibited significantly improved global rigidity, with RMSD values consistently below 1.5 Å (Fig. S30). This global stabilization can be attributed to the central positioning of ReO_4^- which is encapsulated within the β-CD cavity (Fig. 6a), where it forms multiple water-mediated contacts with the hydroxyl binaphthol linker, fostering a more compact and symmetric macrocyclic structure.

Altogether, these findings provide strong evidence that ReO_4^- not only induces specific conformational changes but also stabilizes the overall architecture of **2b**. In contrast, Cl^- functions mainly as a charge-balancing counterion, exerting negligible structural influence. These insights support the conclusion that ReO_4^- actively contributes to the chiroptical sensing mechanism by enabling and stabilizing water-modulated conformers. Moreover, the fact that ReO_4^- cannot penetrate the CD cavity deeply, but barely fits its wider rim, let us infer that the selectivity observed between **2a** and **2b** is related to a size-exclusion effect.

ECD calculations were performed for representative structures of **2b** extracted from both MD simulations: $[H_2(\mathbf{2b})]^{2+}$ from **MD1** and $[H_2(\mathbf{2b})]^{2+}\cdot ReO_4^-\cdot H_2O$ complex from **MD2**. A chromophoric fragment composed of the binaphthol moiety, with two $-CH_2-NH_2^+-CH_3$ substituents at 3,3′ positions, was extracted from several frames of **MD1** corresponding to values of θ dihedral ranging from −75° to −90° (see SI). The structures were reoptimized with DFT at B3LYP/6-31G(d,p) level, including IEF-PCM solvent model for water, and keeping frozen both the value of angle θ and the coordinates of C atoms of the remote CH_3 groups to preserve the overall arrangement obtained by MD. ECD spectra were calculated with TD-DFT at CAM-B3LYP/def2-TZVP and B3LYP/def2-TZVP levels, including IEF-PCM solvent model for water. The calculated spectra for selected representatives from clusters with θ = −75° and −81° are very similar and consist of an intense negative couplet in region of ^1B_b transitions around 230 nm, and a positive band at longer wavelengths due to ^1L_a and ^1L_b transitions (Fig. S35). The representative from cluster with θ = −90° yielded a similar yet less intense ^1B_b couplet. Overall, the spectra reproduce well those measured for **2b** in acidic water, with B3LYP providing the best agreement in the long-wavelength region and CAM-B3LYP in the short-wavelength region (Fig. 7 and S35). Thus, MD and ECD calculations ultimately proof the preferred conformation assumed by the (a*R*)-binaphthol moiety in $[H_2(\mathbf{2b})]^{2+}$, with a dihedral angle around −80°.

The same procedure described above was employed for ECD calculations of $[H_2(\mathbf{2b})]^{2+}\cdot ReO_4^-\cdot H_2O$ complex extracted from **MD2**. In this case, in addition to angle θ and remote C atoms, the coordinate of Re atom was also frozen; moreover, it

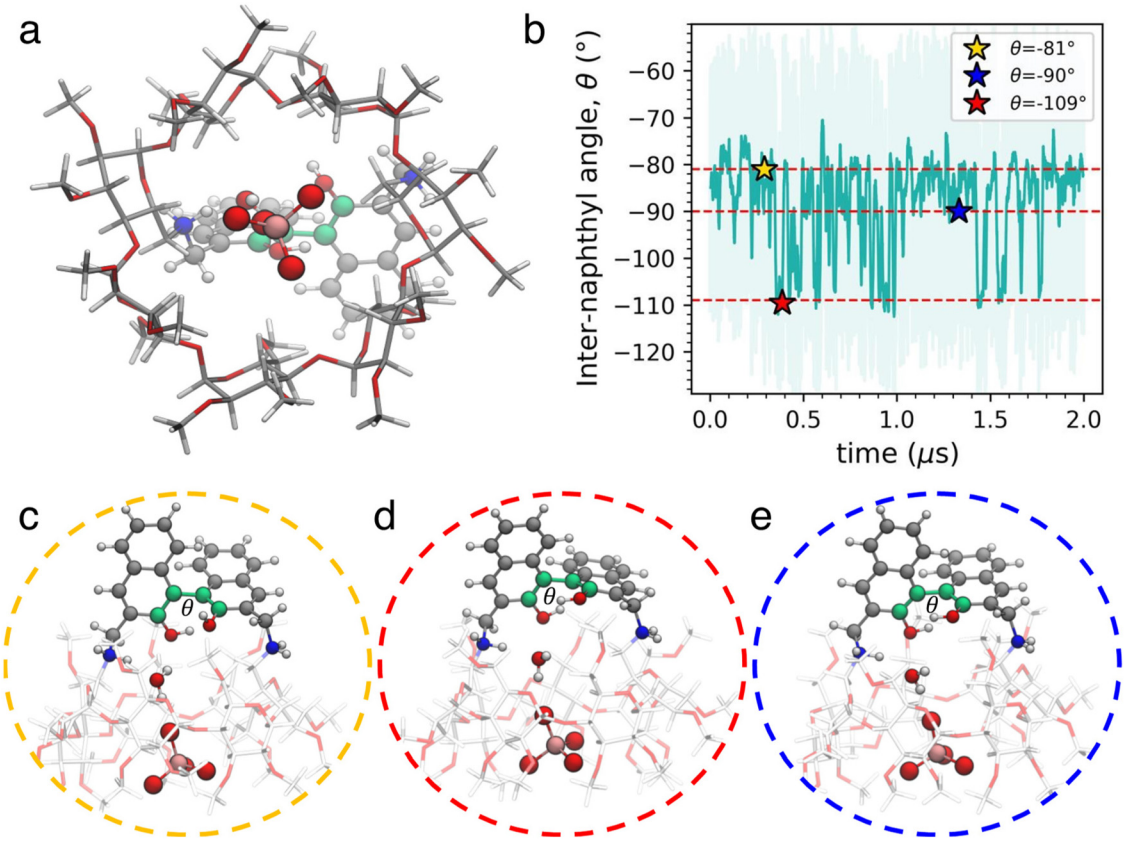

Fig. 6 Molecular dynamics (MD) simulation of binaphthol-bridged CD in the presence of ReO_4^- ion, $[H_2(\mathbf{2b})]^{2+}\cdot ReO_4^-$. (a) Representative structure showing the ReO_4^- ion positioned centrally within the CD cavity. (b) Time evolution of the inter-naphthyl angle (θ) over a 2.0 μs MD simulation. (c–e) Snapshots corresponding to inter-naphthyl angles of −81°, −90°, and −110°, respectively. Water molecules mediating the interaction between ReO_4^- and the binaphthol moiety are shown. Points corresponding to the representative structures in (c–e) are highlighted as stars in (b). All structural representations were generated using VMD (Visual Molecular Dynamics).[23]

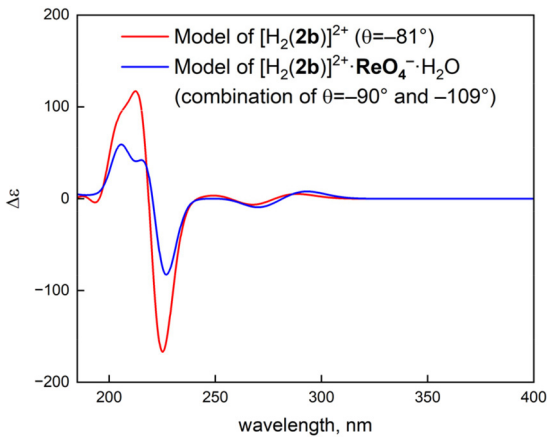

Fig. 7 ECD spectra calculated at the CAM-B3LYP/def2-TZVP level with PCM for water on the chromophoric fragments of compound $[H_2(\mathbf{2b})]^{2+}$ and $[H_2(\mathbf{2b})]^{2+}\cdot ReO_4^-\cdot H_2O$ obtained after **MD1** and **MD2** runs, respectively. For the former, a single conformer with θ = −81° was used; for the latter, a 9 : 1 combination of 2 conformers with θ = −90° and −109° with was used. Plotting parameters: σ = 0.2 eV; scaling factor 2.5 for both spectra.

was necessary to keep a water molecule between the BINOL moiety and ReO_4^- to achieve convergence. Optimizations were run with functional B3LYP, 6-31G(d,p) basis sets for all atoms except Re, SDD basis set for Re with the related MWB60 effective core potential, and including IEF-PCM solvent model for water. Calculations run on representatives from clusters with θ = −90° and −109° (Fig. 6b) showed ECD couplets of opposite sign in the ^1B_b region (Fig. S36), in agreement with the well-known dependence of the couplet sign on θ angle for 1,1′-binaphthyls.[15] Therefore, the presence of a small but non-negligible conformational population with $\theta \approx -110°$ is expected to reduce the overall intensity of the couplet.

In Fig. 7 we compare the spectra calculated on the chromophoric models extracted from **MD1** and **MD2** simulations. For $[H_2(\mathbf{2b})]^{2+}$, the representative from the cluster with θ = −81° was used, whereas for $[H_2(\mathbf{2b})]^{2+}\cdot ReO_4^-\cdot H_2O$ the representatives of the two clusters θ = −90° and −109° were combined with a 9 : 1 proportion.

Although simplified, the approach is able to capture the main changes observed in the ECD spectrum of compound **2b** in acidic conditions upon complexation of ReO_4^- (Fig. 4, top), including a reduction of ^1B_b couplet intensity by 50% (experi-

mentally, 45%) and substantially unchanged signal in the long-wavelength region. ECD spectra calculated on $[H_2(\mathbf{2b})]^{2+}\cdot ReO_4^-\cdot H_2O$ clusters after removing H_2O and ReO_4^- units do not change appreciably (Fig. S37). Natural transition orbitals analysis (NTO) further demonstrates the similar nature of the main transitions responsible for ECD bands of the two model systems, apart from a lift of degeneracy for the two naphthalene rings in $[H_2(\mathbf{2b})]^{2+}\cdot ReO_4^-\cdot H_2O$ (Fig. S37–S40). Therefore, the main conclusion from the computational analysis is that the major chiroptical effect of ReO_4^- binding to **2b** is structural rather than electronic, as the widening of the upper rim makes a new family of conformations accessible to the binaphthol moiety with larger angles θ and less intense or even oppositely signed couplets.

Finally, additional MD simulations and ECD calculations were run on a neutral **2b** system without counterions (**MD3**) as a model of basic conditions. In this case, further conformational space was accessible to the CD scaffold, witnessed by RMSD values often approaching 4 Å (Fig. S30). More importantly, angle θ assumed values between −90° to −100°, eventually stabilizing at ≈−105° (Fig. S32). ECD calculations run on snapshots with θ = −100°, −102° and −108° all yielded positive ECD couplets in the ^1B_b region (Fig. S38), on a par with the pH-dependent evolution of ECD spectra (see Fig. 3).

Conclusions

We have synthesized two-level molecular structures comprising CDs (point chirality) and binaphthyls (axial chirality) as bridging units. Unlike our previous work involving CDs capped with stereodynamic biphenyls, such structures can exhibit an unfavorable stereocommunication mode ('chiral mismatch'), as observed in bridged β-CD **2b**. This occurs because the configuration of the enantiostable binaphthyl (a*R*) cap opposes the preferred configuration imposed by the CD cavity when intramolecular hydrogen bonds are present. Consequently, these structures display highly responsive chiroptical behavior. Notably, **2b** functions as a pH-controlled, single-molecule chiroptical switch, as the optical activity of the binaphthyl unit's exciton couplet undergoes nearly complete reversal from acidic (pH 3) to basic (pH 9) conditions in a fully reversible manner. Additionally, the same host molecule demonstrates a pronounced chiroptical response to perrhenate in aqueous solution at pH 2.5, showing excellent selectivity for this specific anion. The induced strain is confirmed upon comparison with the behaviour of the cavity-free analogue **3** under otherwise identical conditions. Computational analysis confirmed that the major chiroptical effect of ReO_4^- binding to **2b** is structural rather than electronic, making new conformations accessible to the binaphthol moiety with a large variation of the associated dihedral angles.

These remarkable chiroptical properties rely on finely tuned stereochemical communication between the two molecular components—β-cyclodextrin and binaphthyl. We believe the principles demonstrated by these systems can inspire the design of new tailor-made, cyclodextrin-based supramolecular cavities. Moreover, they highlight how stereocommunication between point-chiral cyclodextrins and axially chiral atropoisomeric caps—an aspect previously underexplored—can enable the development of novel functional chiral organic materials, with promising potential in chemosensing. Given the outstanding chiroptical responses of the molecular systems described in this paper, and their modular supramolecular cavities, applications in programmable optical encryption and asymmetric catalysis will be explored in the near future.

Author contributions

Conceptualization: Gi. Pr., D. A and D. P. Formal analysis: Gi. Pr., S. L. C., L. P.-G., Ge. Pe. and V. A. Funding acquisition: D. A. and D. P. Investigation: Gi. Pr., S. L. C. and L. P.-G. Methodology: all authors. Project administration: D. A. and D. P. Supervision: V. A., D. A. and D. P. Writing – original draft: Gi. Pr. Writing – review & editing: Ge. Pe., V. A., D. A., and D. P.

Conflicts of interest

There are no conflicts to declare.

Data availability

The data supporting this article have been included as part of the SI: experimental procedures for the synthesis of derivatives **1–3** and their full characterization, additional UV/vis, ECD and NMR data. See DOI: **https://doi.org/10.1039/d5qo00910c**.

Acknowledgements

Dario Pasini and Giovanni Preda gratefully acknowledge Regione Lombardia (POR FESR 2014-2020-Call HUB Ricerca e Innovazione, Progetto 1139857 CE4WE: Circular Economy for Water and Energy), and Ministero dell'Università e della Ricerca (MUR) through the program "Dipartimenti di Eccellenza 2023–2027" and the University of Pavia for financial support. Dario Pasini thanks the Région Grand Est and the Eurométropole de Strasbourg for the award of a Gutenberg Excellence Chair. Dominique Armspach gratefully acknowledges financial support by the "Cercle Gutenberg". Valeria Amendola and Sonia La Cognata gratefully acknowledge financial support from the Italian Ministero dell'Università e della Ricerca (MUR) under the PRIN 2022 call (Prot. 20224HH9KP, project MUR: 20224HH9KP_002). We thank Daniele Feltri (University of Pavia) for the synthesis of model compound **3** and Dr Lorenzo Cupellini for assistance with the computations. Gennaro Pescitelli and Laura Pedraza-González gratefully acknowledge the University of Pisa for the availability of high-performance computing resources and support of the computing service at the University of Pisa. Valeria Amendola

and Dario Pasini thank Teresa Recca and Barbara Mannucci of Centro Grandi Strumenti NMR and MS Facility for their support and assistance in this work.

References

1 F. Begato, G. Licini and C. Zonta, Exploiting Chirality in Confined Nanospaces, *Angew. Chem., Int. Ed.*, 2023, **62**, e202311153.

2 G. Crini, Review: A History of Cyclodextrins, *Chem. Rev.*, 2014, **114**, 10940–10975.

3 (*a*) L. Zhang, H.-X. Wang, S. Li and M. Liu, Supramolecular chiroptical switches, *Chem. Soc. Rev.*, 2020, **49**, 9095–9120; (*b*) G. Preda and D. Pasini, One-Handed Covalent Helical Ladder Polymers: The Dawn of a Tailorable Class of Chiral Functional Materials, *Angew. Chem., Int. Ed.*, 2024, **63**, e202407495; (*c*) Y.-Y. Zhao, Z.-Q. Li, Z.-L. Gong, S. Bernhard and Y.-W. Zhong, Endowing Metal-Organic Coordination Materials with Chiroptical Activity by a Chiral Anion Strategy, *Chem. – Eur. J.*, 2024, **30**, e202400685.

4 B. L. Feringa, R. A. van Delden, N. Koumura and E. M. Geertsema, Chiroptical Molecular Switches, *Chem. Rev.*, 2000, **100**, 1789–1816.

5 (*a*) D. Sahoo, R. Benny, N. K. Ks and S. De, Stimuli-Responsive Chiroptical Switching, *ChemPlusChem*, 2022, **87**, e202100322; (*b*) A. Nitti and D. Pasini, Aggregation-Induced Circularly Polarized Luminescence: Chiral Organic Materials for Emerging Optical Technologies, *Adv. Mater.*, 2020, **32**, 1908021; (*c*) P. T. Probst, Y. Dong, Z. Zhou, O. Aftenieva and A. Fery, Bottom-Up Assembly of Inorganic Particle-Based Chiroptical Materials, *Adv. Opt. Mater.*, 2024, **12**, 2301834; (*d*) W. Ma, H. Kuang, L. Xu, L. Ding, C. Xu, L. Wang and N. A. Kotov, Attomolar DNA detection with chiral nanorod assemblies, *Nat. Commun.*, 2013, **4**, 2689.

6 D. Armspach, D. Matt and N. Kyritsakas, Anchoring a Helical Handle across a Cavity: The First 2,2′-Bipyridyl-Capped α-Cyclodextrin Capable of Encapsulating Transition Metals, *Polyhedron*, 2001, **20**, 663–668.

7 M. Kazem-Rostami, A. Orte, A. M. Ortuño, A. H. G. David, I. Roy, D. Miguel, A. Garci, C. M. Cruz, C. L. Stern, J. M. Cuerva and J. F. Stoddart, Helically Chiral Hybrid Cyclodextrin Metal–Organic Framework Exhibiting Circularly Polarized Luminescence, *J. Am. Chem. Soc.*, 2022, **144**, 9380–9389.

8 M. Ménand, M. Sollogoub, B. Boitrel and S. Le Gac, Hexaphyrin–Cyclodextrin Hybrids: A Nest for Switchable Aromaticity, Asymmetric Confinement, and Isomorphic Fluxionality, *Angew. Chem., Int. Ed.*, 2016, **55**, 297–301.

9 (*a*) H. Shigemitsu, K. Kawakami, Y. Nagata, R. Kajiwara, S. Yamada, T. Mori and T. Kida, Cyclodextrins with Multiple Pyrenyl Groups: An Approach to Organic Molecules Exhibiting Bright Excimer Circularly Polarized Luminescence, *Angew. Chem., Int. Ed.*, 2022, **61**, e202114700; (*b*) S. Dash, A. Fihey, L. Favereau, C. Lagrost, R. Benchouaia, S. Blanchard, M. Ménand and S. Le Gac, Encoding and Expressing the Handedness of a Möbius π System in a Totemic Architecture, *J. Am. Chem. Soc.*, 2025, **147**, 15242–15252.

10 R. Benchouaia, N. Cisse, B. Boitrel, M. Sollogoub, S. Le Gac and M. Menand, Orchestrating Communications in a Three-Type Chirality Totem: Remote Control of the Chiroptical Response of a Möbius Aromatic System, *J. Am. Chem. Soc.*, 2019, **141**, 11583–11593.

11 G. Preda, S. Jung, G. Pescitelli, L. Cupellini, D. Armspach and D. Pasini, Enabling Stereochemical Communication and Stimuli–Responsive Chiroptical Properties, *Chem. – Eur. J.*, 2023, **29**, e202302376.

12 (*a*) P. K. Baruah, R. Gonnade, P. R. Rajamohanan, H.-J. Hofmann and G. J. Sanjayan, BINOL-Based FoldamersAccess to Oligomers with Diverse Structural Architectures, *J. Org. Chem.*, 2007, **72**, 5077–5084; (*b*) L. Di Bari, G. Pescitelli and P. Salvadori, Conformational Study of 2,2′-Homosubstituted 1,1′-Binaphthyls by Means of UV and CD Spectroscopy, *J. Am. Chem. Soc.*, 1999, **121**, 7998–8004; (*c*) M. Caricato, C. Coluccini, D. Dondi, D. A. Vander Griend and D. Pasini, Nesting Complexation of C_{60} with Large, Rigid D_2 Symmetrical Macrocycles, *Org. Biomol. Chem.*, 2010, **8**, 3272–3280; (*d*) M. Caricato, N. J. Leza, K. Roy, D. Dondi, G. Gattuso, L. S. Shimizu, D. A. Vander Griend and D. Pasini, A Chiroptical Probe for Sensing Metal Ions in Water, *Eur. J. Org. Chem.*, 2013, 6078–6083; (*e*) M. Caricato, A. Olmo, C. Gargiulli, G. Gattuso and D. Pasini, A "clicked" macrocyclic probe incorporating Binol as the signalling unit for the chiroptical sensing of anions, *Tetrahedron*, 2012, **68**, 7861–7866; (*f*) M. Agnes, A. Nitti, D. A. Vander Griend, D. Dondi, D. Merli and D. Pasini, A chiroptical molecular sensor for ferrocene, *Chem. Commun.*, 2016, **52**, 11492–11495; (*g*) C. Coluccini, D. Dondi, M. Caricato, A. Taglietti, M. Boiocchi and D. Pasini, Structurally-Variable, Rigid and Optically-Active D_2 and D_3 Macrocycles Possessing Recognition Properties towards C_{60}, *Org. Biomol. Chem.*, 2010, **8**, 1640–1649; (*h*) D. Pasini and A. Nitti, Recent Advances in Chirality Sensing using Atropoisomeric Molecular Receptors, *Chirality*, 2016, **28**, 116–123.

13 (*a*) D. Armspach and D. Matt, Metal-Capped α-Cyclodextrins: Squaring the Circle, *Inorg. Chem.*, 2001, **40**, 3505–3509; (*b*) D. Armspach and D. Matt, The tris(4-tert-butylphenyl)methyl group: a bulky substituent for effective regioselective difunctionalisation of cyclomaltohexaose, *Carbohydr. Res.*, 1998, **310**, 129–133.

14 D. Verga, M. Nadai, F. Doria, C. Percivalle, M. Di Antonio, M. Palumbo, S. N. Richter and M. Freccero, Quinone Methides Tethered to Naphthalene Diimides as Selective G-Quadruplex Alkylating Agents, *J. Am. Chem. Soc.*, 2010, **132**, 14625–14637.

15 (*a*) S. F. Mason, R. H. Seal and D. R. Roberts, Optical activity in the biaryl series, *Tetrahedron*, 1974, **30**, 1671–1682; (*b*) C. Rosini, S. Superchi, H. W. I. Peerlings and E. W. Meijer, Enantiopure Dendrimers Derived from the 1,1′-Binaphthyl Moiety: A Correlation Between Chiroptical

Properties and Conformation of the 1,1′-Binaphthyl Template, *Eur. J. Org. Chem.*, 2000, 61–71; (*c*) G. Pescitelli, ECD exciton chirality method today: a modern tool for determining absolute configurations, *Chirality*, 2022, **34**, 333–363.

16 (*a*) P. E. Reyes-Gutiérrez, M. Jirasek, L. Severa, P. Novotna, D. Koval, P. Sazelova, J. Vavra, A. Meyer, I. Cisarova, D. Saman, R. Pohl, P. Stepanek, P. Slavicek, B. J. Coe, M. Hajek, V. Kasicka, M. Urbanova and F. Teply, Functional helquats: helical cationic dyes with marked, switchable chiroptical properties in the visible region, *Chem. Commun.*, 2015, **51**, 1583–1586; (*b*) W. Lu, G. Du, K. Liu, L. Jiang, J. Ling and Z. Shen, Chiroptical Inversion Induced by Rotation of a Carbon–Carbon Single Bond: An Experimental and Theoretical Study, *J. Phys. Chem. A*, 2014, **118**, 283–292; (*c*) N. Saleh, B. Moore, M. Srebro, N. Vanthuyne, L. Toupet, J. A. G. Williams, C. Roussel, K. K. Deol, G. Muller, J. Autschbach and J. Crassous, Acid/Base-Triggered Switching of Circularly Polarized Luminescence and Electronic Circular Dichroism in Organic and Organometallic Helicenes, *Chem. – Eur. J.*, 2015, **21**, 1673–1681.

17 (*a*) J. W. Canary, Redox-triggered chiroptical molecular switches, *Chem. Soc. Rev.*, 2009, **38**, 747–756; (*b*) Z. Dai, J. Lee and W. Zhang, Chiroptical Switches: Applications in Sensing and Catalysis, *Molecules*, 2012, **17**, 1247–1277.

18 L. A. Paquette and J. M. Gardlik, Utilization of Buttressing Effects for Comparing Ring Inversion and π Bond Shifting Transition State Geometries in Cyclooctatetraenes, *J. Am. Chem. Soc.*, 1980, **102**, 5033–5035.

19 S. P. Cornes, M. R. Sambrook and P. D. Beer, Selective perrhenate recognition in pure water by halogen bonding and hydrogen bonding alpha-cyclodextrin based receptors, *Chem. Commun.*, 2017, **53**, 3866–3869.

20 R. Mobili, G. Preda, S. La Cognata, L. Toma, D. Pasini and V. Amendola, Chiroptical sensing of perrhenate in aqueous media by a chiral organic cage, *Chem. Commun.*, 2022, **58**, 3897–3900.

21 V. Amendola, G. Bergamaschi and A. Miljkovic, Azacryptands as molecular cages for anions and metal ions, *Supramol. Chem.*, 2018, **30**, 236–242.

22 R. Alberto, G. Bergamaschi, H. Braband, T. Fox and V. Amendola, $^{99}TcO_4^-$: Selective Recognition and Trapping in Aqueous Solution, *Angew. Chem., Int. Ed.*, 2012, **51**, 9772–9776.

23 W. Humphrey, A. Dalke and K. Schulten, VMD: visual molecular dynamics, *J. Mol. Graphics*, 1996, **14**, 33–38.